

Steady-State Operation of Tokamaks: Key Physics and Technology Developments on Tore Supra

J. Jacquinet
on behalf of the Tore Supra Team

Association Euratom-CEA, CEA Cadarache, CEA-DSM-DRFC,
F-13108 S^t Paul lez Durance, France

e-mail contact: jean.jacquinet@cea.fr

Abstract. Important technological and physics issues related to long pulse operation required for a reactor are now being addressed in Tore Supra. experimental results in conditions where all the plasma facing components are actively cooled during pulses exceeding six minutes. Important physics issues related to continuous operation are observed in non inductively driven plasmas.

1. Introduction

Most of present-day experiments can provide fusion plasmas with duration long enough to study MHD, heat and particle transport phenomena. These plasmas are however marginal for addressing current diffusion physics particularly in the large devices, and all of them are much too short to study wall erosion and hydrogen saturation. Nevertheless, long pulse research has been performed on JT60-U [1] and TRIAM-1M [2] in Japan and on the European tokamak JET [3]. Plasma duration is generally limited either by the primary transformer or by inadequately cooled plasma facing components (PFCs) that can accumulate only a limited amount of heat. Cost effective continuous operation requires therefore superconducting magnets, non-inductive current drive, particle control and actively cooled PFCs.

ITER [4] is designed to operate close to ignition. It should produce a fusion power of 500 MW, corresponding to a fusion gain $Q=5-10$. It also aims at steady state operation. Several devices are now also designed for long pulse experiments using superconducting coils: EAST, JT60-SC, KSTAR, SST-1 and W7-X. Tore Supra is the largest superconducting tokamak in operation, equipped with actively cooled PFCs and with a full set of radio frequency (RF) heating and current drive systems. It is currently in a unique position to explore relevant issues relating to continuous operation, especially on the technology of actively cooled components and the physics of long pulse operation with non-inductive current drive. Significant progress has been recorded at Tore Supra, in terms of plasma duration and injected energy:

2 min/280 MJ in 1996; 4 min/740 MJ in 2002 and in 2003, an energy of 1 GJ has been injected into plasmas lasting more than 6 minutes (Fig. 1) [5].

This paper gives an overview of the recent Tore Supra results. Technology developments of cooled PFCs, RF heating systems including surveillance infrared cameras for high power and long pulse operation are presented. A detailed account on exhaust power flux on PFCs and on the particle balance is reported. We address the physics issues linked to full non-inductive current operation, where new phenomena can develop over very long time scales. The impact of the Tore Supra experiment results on extrapolation to ITER are also discussed.

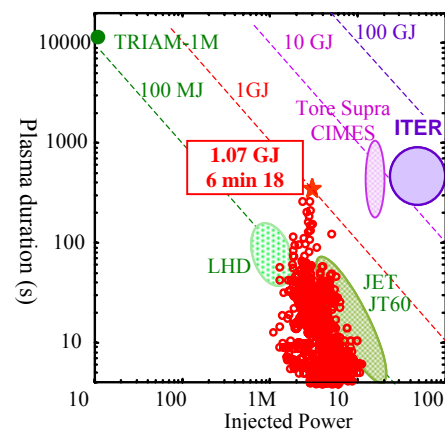


Fig. 1: Progress in Tore Supra and in other devices. "CIMES" indicates the domain to be explored with the heating and CD systems upgrade now ongoing on Tore Supra [6].

2. Technology developments for steady-state operation

Continuous operation in tokamaks requires:

- superconducting magnets to limit the energy consumption to a reasonable level;
- long pulse capability of heating and current drive systems;
- cooled PFCs able to handle the injected power, and ultimately the fusion power;
- long pulse capability means for fuelling and pumping the discharge;
- diagnostics and real time (RT) plasma control using specific feedback algorithms.

These conditions are now met in Tore Supra. Indeed, it is equipped with superconducting magnets cooled by superfluid helium at 1.8 K which have been operating with high reliability for 16 years. Other installations of much larger size, such as CEBAF (USA) and the LHC project (CERN), are based on the innovative technology of the Tore Supra cryo-magnetic system.

2.1 Actively cooled plasma facing components

All the in-vessel components of Tore Supra have been replaced in 2000-2001. They are actively cooled by a primary high temperature, pressurized water loop (120°C, 30 bars, 980 m³/h) [7]. The main part of the upgrade was the installation of a toroidal pumped limiter (TPL) with a heat exhaust capability of 15 MW at a peak power density of about 10 MWm⁻². A set of 10 actively cooled neutralizers are installed below the TPL. The peak heat flux on these neutralizers can reach 15 MWm⁻². The TPL is made up of 574 individually-cooled elements covering an area of 7.6 m². It has been installed with a positional accuracy of about 1 mm to ensure an even distribution of the heat load. Each of the TPL elementary components is armoured with 21 tiles made of carbon fibre composite (CFC) bonded by Active Metal Casting technique (AMC[®]) to a water-cooled heat sink made of CuCrZr [8]. The typical time constant for thermal diffusion is a few seconds. The entire vacuum vessel is also actively cooled with high temperature pressurized water (up to 200°C/30 bar), allowing to remove up to 10 MW of radiated power (peak power density 1 MWm⁻²). It is worth noting that ITER will also have to run under steady-state conditions with active cooling of all internal systems. The experience gained at Tore Supra on actively cooled PFCs will be applicable to ITER; for example, the technologies for the ITER vertical divertor target. This experience is essentially due to the undertaking of a comprehensive R&D and industrialization of the PFCs. Development of specific acceptance test, repair capability during manufacturing and many insights on the material specifications have been studied and carefully recorded [9].

2.2 Actively cooled thermography and robotics for PFC control

The PFC temperatures are monitored by a set of seven actively cooled infrared (IR) endoscopes (Fig. 2a). The IR thermographic system has been designed to oversee the entire surface of the TPL and five RF antennae [10]. Each endoscope (2.5 m long) is equipped with 3 viewing lines: 2 IR cameras able to survey 2 x 35° of the TPL and 1 RF antenna). New generation digital cameras are used for real time control against overheating. The system resolution is about 9 mm, allowing to control the surface temperature of the smallest PFC elements (20 mm) with an error < 10%. Infrared endoscopes for JET and ITER are also being developed at Cadarache [11]. The part of the viewing line which is close to the plasma is made of actively cooled mirrors designed

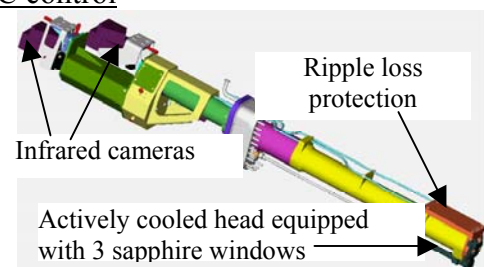


Fig. 2a : Actively cooled endoscopes.

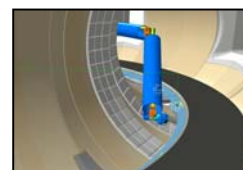


Fig. 2b: An AIA with ITER dimensions (segments, 8m long) developed at Tore Supra.

to withstand fusion power. In order to provide in-vessel inspection and maintenance of the facility, the design, manufacture and testing of an Articulated Inspection Arm (AIA) are ongoing at Cadarache. The AIA (Fig. 2b) will be, in 2006 [12], capable of performing inspections with a load of 10 kg in the Tore Supra temperature and vacuum tokamak environment.

2.3 Heating and current drive systems

Tore Supra is equipped with three RF systems: i) lower hybrid current drive (LHCD), 3.7 GHz/8 MW klystron power; ii) ion cyclotron resonance heating (ICRH), 30-80 MHz/12 MW generator power; iii) electron cyclotron resonance heating (ECRH) 118 GHz/0.8 MW gyrotron power.

A long pulse LH launcher has been implemented in 1999. It can inject a power up to 4 MW, with a power density of 25 MW/m² [13]. Efficient water cooling has allowed to inject more than 2 MW during 375 s without any arcing with a reflection coefficient < 5 %. No pressure increase in the vacuum tank surrounding the launcher has been detected. So far, the LH power is limited by the klystrons installed in 1986 with a full power specification limited to 30 s. A new 3.7 GHz klystron is under development to upgrade the installed power of the Tore Supra transmitters up to 12 MW for 1000 s [14]. The klystron is specified to deliver 750 kW on a matched load, and up to 700 kW with a Voltage Standing Wave Ratio (VSWR) of 1.4. The klystron is equipped with a diode type electron gun, a five cavity RF structure, a single tapered output waveguide equipped with a single BeO RF window and a large diameter hypervapotron collector. Pre-prototype testing has begun. At low duty cycle (10% with 5ms pulse length) an RF output power of 770 kW has been measured. The efficiency is 46.6% and the gain is 54 dB. With a VSWR of 1.4:1, a minimum output power of 660 kW has been measured and the klystron is stable at all phases. In CW operation, the klystron has produced an output power of 680 kW. Limitations have been found due to the body intercepted power. A new prototype tube has been designed to overcome these limitations with the aim to receive the full complement of tubes in 2006. A second launcher based on the new passive-active-multijunction (PAM) antenna is being fabricated [15]. It is designed to radiate 2.7 MW at a power density of 25 MW/m². The design includes features which are mandatory for ITER, such as the possibility to cool actively the plasma facing grill mouth and to withstand high disruption forces. Following successful plasma tests on FTU in the frame of a CEA-ENEA collaboration [16], this type of antenna will now be installed on Tore Supra to study its long pulse behaviour.

A prototype ICRH antenna has been built with the conjugate-T matching circuit, as proposed for ITER and for the JET-EP antenna [17]. A few experiments in 2004 on Tore Supra have shown the importance of the coupling effect between straps, and thus the need for an active control of the current phasing between them. Nevertheless, the load tolerant properties of such a circuit have been observed. The antenna will be reinstalled in 2005 with improved electronic control to further document this type of circuit and prepare for the use of the JET-EP antenna.

A negative ion source and accelerator programme for ITER (1 MeV/ 40 A of D⁻) is on-going at Cadarache [18]. The design specification of the ion source is that it should produce an accelerated D⁻ current density of 200 A/m² with < 1 electron extracted per accelerated D⁻ ion. The ion source must operate at a source pressure of ≤ 0.3 Pa, an injected power ranging between 1 and 2 kW per litre of source volume, during long pulses ≤ 3600 s. 200 A/m² of D⁻ has been demonstrated for short pulse (5 s) operation, under these conditions. A model of the ITER ion source is being tested on the MANTIS test rig at Cadarache. Long pulse operation has been achieved with pulse durations up to 1000 s, with an accelerated D⁻ current density of 90 A/m². The highest negative ion yield during long pulse operation has been 150 A/m², H⁻, with 78 kW (2.6 kW/l) of arc power. A new "ITER-like" accelerator, a down scaled version

of the ITER SINGAP accelerator [19], has been recently built and installed on the Cadarache 1 MV test bed. The objective is to demonstrate reliable D^- beam acceleration as close as possible to 1 MeV with a current density of $\approx 200 \text{ A/m}^2$, and the parameters and beam optics required for ITER. The ITER-like accelerator has already produced 850 keV D^- beams with a current density of 15 A/m^2 . Higher current density D^- beams, 85 A/m^2 have been produced at 580 keV. The beam divergence has been of the order of 3 to 5 mrad.

A new gyrotron for ECRF heating, jointly developed by Association Euratom-CEA/Association Euratom-Confédération Suisse/Association Euratom-FZK/TED (Thales Electron Devices), is being tested at Cadarache [20]. The goal of these tests is to demonstrate an ECRF power of 400 kW for a pulse duration of up to 600 s. If tests are successful, 5 additional gyrotrons will be manufactured and used mainly for current density profile control on Tore Supra. Two gyrotrons (400 kW, < 30s) were available for the experiments reported in the article.

2.4 Fueling systems

Supersonic Molecular Beam Injection modules have been implemented in Tore Supra. They are able to launch a series of very short/dense gas jets at Mach number 5. With this system, a fuelling efficiency of 30% - 60% has been obtained, to be compared with the efficiency of a conventional gas puff of 10% - 15% [21]. In 2003, a new continuous pellet injector was installed [22]. It is based on a screw extruder, cooled by liquid He. This injector can inject pellets continuously at a frequency up to 10 Hz and a velocity between 100 - 600 m/s, with a very high reliability ($\sim 99\%$). The fuelling can be adjusted between 1.5 and 6×10^{20} D atoms by varying the pellet size. Pellets can be injected from four different poloidal locations regularly distributed from the low to the high field side. The system optimizes the fuelling efficiency and density profile control making a compromise between the pellet velocity and the ExB drift [23]. It is also used for studying particle transport and the complex interplay between pellet ablation, current profile and MHD instabilities [24].

Pellet fuelled LH driven discharges lasting up to 2 minutes have been demonstrated [25]. An overall recording of the main parameters of this discharge is shown in Fig. 3. 155 pellets at a frequency close to 1.2 Hz have been injected into the plasma. Each pellet was preceded by a notch of the LH power 30 ms before the arrival of the pellet, in order to avoid rapid pellet ablation by the LH driven fast electrons. RT control kept V_{loop} at a constant value close to zero ($\sim 0.07 \text{ V}$). The plasma line density could be maintained near the target value of $2.5 \times 10^{19} \text{ m}^{-3}$. This result is very encouraging for ITER steady-state operation in the presence of fast particles.

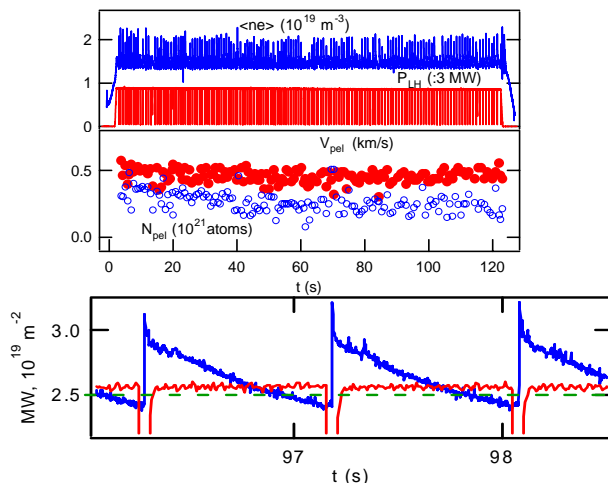


Fig. 3: LH power, volume average density, pellet velocity and number of injected atoms (top). The bottom figure displays the LH power and the central line density together with its pre-programmed target.

2.5 Real time control development

Controlling simultaneously plasma parameters, PFC temperature and heating systems is a major issue for steady-state operation. A new full RT control is now available in Tore Supra including current profile and plasma equilibrium reconstruction [26]. RT treatment of various diagnostics (hard X-ray tomography, interfero-polarimetry, metallic impurities,

superheterodyne radiometer, and IR cameras surveillance) is used to prevent MHD instabilities and overheating of PFCs and RF antennae. Plasma equilibrium reconstruction is performed routinely using a finite element method implemented in C++ to solve the Grad-Shafranov equation. With these tools, steady-state discharges at zero loop voltage have been achieved, controlling both plasma position and shape within a few millimetres, a key issue for RF wave coupling. Specific algorithms based on impurity measurements have been developed and are continuously used to switch off momentarily the LH power during arcing. A feedback on the heating power yields active control of the PFCs heat load. Finally, control of the LH power profile deposition is available taking advantage of the hard X-ray tomography, thus allowing some active control of the current profile. A further development is to better constrain the RT equilibrium by including the pressure profile from interferometry and the superheterodyne radiometer.

Associated to these control tools, specific RT algorithms dedicated to the device safety have been implemented and are routinely working.

3. Key experimental results

3.1 One Giga-Joule injected into the plasmas

Long pulse Tore Supra experiments have been carried out using LHCD, with toroidal field $B_T = 3.4$ T, plasma current $I_p = 0.5-0.7$ MA, and density $n_e(0) \leq 3 \times 10^{19} \text{ m}^{-3}$. The accessible range of I_p and density is presently limited by the available LH power. B_T was optimized to avoid MHD instabilities in these conditions. Sawtooth free plasmas - characterized by a central safety factor $q(0)$ between $1.5 - 2$, $T_e(0) \sim 5$ keV, $T_i(0) \sim 1.5$ keV- were obtained maintaining zero loop voltage and constant current by a RT control.

Figure 4 illustrates a discharge performed at 0.5 MA with an injected energy of 1.07 GJ. The neutron flux was constant during the discharge, confirming very stable density, temperature and impurity content over six minutes ($Z_{\text{eff}} \sim 2$). This discharge exhibited the features of the so-called Lower Hybrid Enhanced Performance (LHEP) regime [27]. Peaked electron temperature profile ($T_e(0) = 4.65$ keV) was observed together with an enhancement of energy confinement, correlated with a high value of inductance ($l_i = 1.45$) and a negative magnetic shear within a narrow core region ($r/a < 0.2$). The improvement factor (H_L), with respect to the ITER L-mode scaling [28], is about 1.35.

No MHD instabilities were observed over 250 s. At $t = 252$ s, a high level of metallic impurities, due to arcings in the LH waveguides, was detected. In consequence, the LH power was lowered by RT control to avoid disruption and damaging the LH launcher. The plasma with acceptable metallic impurities was immediately recovered. However, after this event, the 3/2 MHD activity localized near the plasma center developed (see $T_e(0)$ and neutron signals in Fig. 4), which did not affect the global energy confinement. This example shows clearly that integrated RT control of device safety and plasma equilibrium is essential for continuous operation.

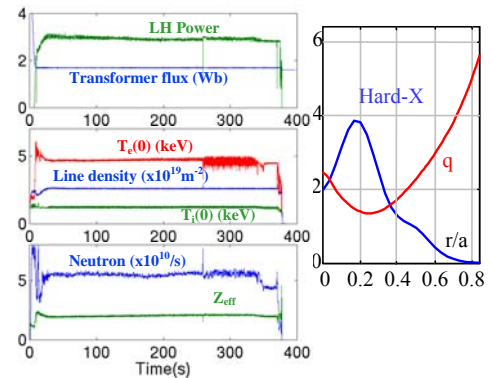


Fig. 4: Discharge with injected energy of 1 GJ. q -profile at $t = 120$ s, obtained from CRONOS [29] calculation including the hard X-ray (60-80 keV) and polarimetry measurements.

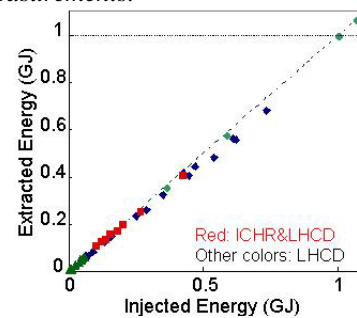


Fig. 5 : Energy balance from calorimetry

The IR cameras indicated that the surface temperature of PFCs reached a stable value after a few seconds. An increase of 3°C was observed with a good toroidal repartition, corresponding to the removal of 1.5 MW (~50% of total input power). A complete energy balance by calorimetric measurements has also been performed (Fig. 5). More than 98% of the energy is accounted for with approximately 50% on the TPL, 25% on the first wall panels (75 m² with the bumpers) and 25% shared between the outboard limiter and antennas. The largest part of this last portion is absorbed by the cooled LH launcher, which provided more than 70% of the injected power and is mainly related to RF losses in the launcher itself. About 2-3% of the total is lost through fast electrons (100 keV), trapped in the magnetic ripple wells and impinging on port edges between the toroidal magnetic coils.

3.2 Particle balance

The in-vessel deuterium (D) inventory has been evaluated [30]. A large D retention rate (Φ_{iv}) was observed. Approximately, half of the injected particle flux is recovered in the pumps and the rest is implanted into the in-vessel components[5]. Fig. 6 shows the time evolution of Φ_{iv} during three consecutive long discharges without conditioning procedure. Φ_{iv} is found to be identical for these discharges, and the retention shows no sign of saturation after more than 6 plasma minutes, or 15 minutes of cumulative plasma time. Initially ($t < 100$ s), Φ_{iv} is seen to decrease before reaching a stationary value, typically of 2×10^{20} D/s. In the stationary phase, the in-vessel inventory becomes simply proportional to the shot duration; so far the highest value is 7.8×10^{22} D. The amount of excess particles initially trapped is found to be correlated with the amount of particles recovered after the shot ($\sim 2-5 \times 10^{21}$ D). It is therefore associated with a transient retention mechanism, while the stationary value corresponds to a permanent retention mechanism. Several processes have been examined to explain this observation. A progressive saturation of the surfaces bombarded by energetic charge exchange neutrals could be compatible with the experimental retention rate during the first phase, but cannot explain the identical shot to shot behaviour, as the implanted surfaces should remain saturated between shots. A transient trapping of D particles into the porosity of the CFC is a potential candidate to explain the behaviour of Φ_{iv} during the first phase. For the stationary phase, codeposition of deuterium with carbon, due to chemical erosion generating hydrocarbons, has been invoked. However, the carbon source needed to account for the experimental retention rate seems to be higher than what is observed in terms of redeposited layers in the machine [31]. Therefore it seems difficult to explain large retention with codeposition alone.

Particle recovery after disruptions, as suggested for ITER, has also been studied. It can be significant when the plasma current exceeds a threshold, as predicted in Ref [32], approximately 0.8 MA in Tore Supra [30]. Above this threshold, after a disruption, the recovered quantity of deuterium can reach up to 50-100 Pam³ for $I_p > 0.8$ MA ($2.5-5 \times 10^{22}$ D, i.e., ten times higher than the usual recovery after the shot). However, this quantity remains moderate compared to the in-vessel inventory accumulated over a full day of long discharges. Dedicated experiments are being investigated to accurately evaluate the process in terms of particle recovery, specially using Helium Massive Injection, designed to mitigate runaway electrons during disruptions [33].

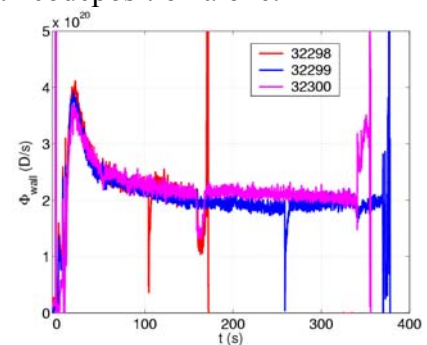


Fig. 6: In-vessel retention rate for 3 consecutive long discharges.

3.3 MHD stability

In fully non-inductive discharges, it is frequently observed that even after several minutes a bifurcation occurs into a regime in which a strong permanent MHD activity develops. This so-called MHD regime [34] degrades fast electron confinement as well as LHCD efficiency and confinement in the plasma core. In these discharges, the current profile is globally peaked, but hollow in the narrow core region $r/a \leq 0.2$ (Fig. 4). A map of the resistive MHD properties has been drawn as a function of B_T , I_p and the parallel index of the LH waves ($N_{//}$). Linear stability properties show the existence of stable domains for $q_{\min} > 2$ and for q_{\min} just above unity. However, most of the considered discharges are linear MHD unstable. In several cases, saturated tearing modes are observed without deleterious effects. These effects, i.e. the MHD regime, are only triggered by full reconnection of double tearing modes, whose condition of occurrence can be estimated from the calculation of the helical flux relative to the resonant surface $q=m/n$: $\psi^* = \int_0^{\bar{\psi}} d\bar{\psi}(1 - nq/m)$.

The full reconnection occurs when $\psi^* \sim 0$ at the outer resonant surface [35], which corresponds approximately to condition: $m/n > q_{\min} > q(\psi_{outer}^* = 0)$. As a result, a map of MHD properties for LHCD driven discharges is established. The domain (B , I_p) where the deleterious MHD regime can be triggered (with $N_{//}=1.7$) is shown in Fig. 7. In this figure, the frontiers of rational q_{\min} and $\psi^*=0$ are obtained from reference discharges. The triggering region is, in fact, for q_{\min} slightly below a rational (as for the record pulses), down to a q -profile where ψ^* is slightly above zero at the outer resonant surface. The drawing of such a map will be implemented in a RT control loop to avoid entering into deleterious MHD regime.

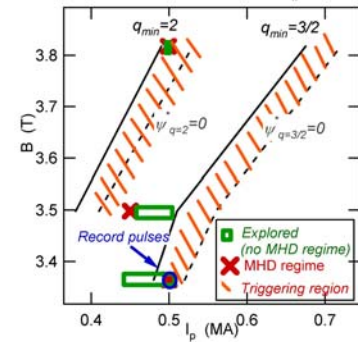


Fig. 7 : Domain (B , I_p) where deleterious MHD regime can be triggered.

3.4 Non-linear oscillations

Several long Tore Supra LHCD discharges exhibited spontaneous regular oscillations of the electron temperature in a narrow core region [36] with a frequency of a few Hz (so-called O-regime). They do not present any helical structure, therefore they cannot be ascribed to any known MHD activity. This phenomenon occurred when the ohmic current was low or nil. It is reproducible and can last several minutes. Understanding this new plasma regime is therefore important for burning plasma experiments in steady-state.

The most plausible explanation is that the plasma current and the electron temperature evolve as a non-linearly coupled predator-prey system. Complex coupling between the electron heat diffusivity (χ_e) and the resistive current diffusion equations is due to: i) dependence of χ_e on the q -profile; ii) dependence of the LHCD efficiency upon both q -profile (wave propagation) and temperature (wave absorption). Integrated modelling performed with the CRONOS code [29] indicates that the O-regime is an uncomplete transition towards an internal transport barrier [37].

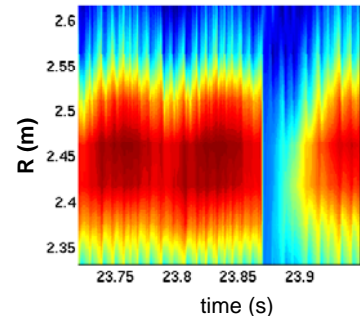


Fig. 8 : Contour plots of T_e

In some cases, these oscillations co-exist with the MHD modes. Therefore, an interplay between the MHD instability and oscillations may occur, since both phenomena are linked to the q profile. An example of slow oscillations (10Hz) superimposed to a faster MHD activity inducing sporadic crashes is shown in Fig. 8. In some cases, MHD-driven reconnection is likely to help in maintaining a flat q -profile, which, in the simulations, is a necessary

condition to trigger the oscillations [37]. RT current profile control seems necessary to maintain the high central temperature.

3.5 Synergy between Electron Cyclotron and Lower Hybrid Current Drive

An improvement of the current drive efficiency of electron cyclotron waves in the presence of LH waves has been predicted by kinetic calculations. This synergy effect can be defined and quantified by $F_{\text{syn}} = (I_{\text{LH+EC}} - I_{\text{LH}})/I_{\text{EC}} > 1$, where $I_{\text{LH+EC}}$ is the current driven by the combination of the two waves, and I_{LH} , I_{EC} are the currents driven by the two waves independently in the same plasma conditions. The effect results from a favourable interplay of the velocity space diffusions induced by the two waves: the EC wave pulling low-energy electrons out of the Maxwellian bulk, and the LH wave driving them to high parallel velocities.

In Tore Supra, dedicated ECCD experiments have been performed in full LHCD discharges [38]. A multiple feedback strategy has been used to obtain discharges at zero loop voltage, constant plasma current and constant average electron density in steady-state. In these conditions, an ECCD pulse up to 10 s has been applied to drive the current in the same direction as the LH current. This technique has allowed a clear demonstration of the synergy effect in steady state conditions. For instance, 500 kW of LHCD have been replaced by 700 kW of ECCD, which implies an efficiency of the same order of magnitude; the ECCD efficiency is generally predicted and observed to be much lower [38]. Analysis yields an ECCD current of about 90 kA, to be compared with the theoretical value of 24 kA obtained with either a toroidal ray-tracing code including the linear ECCD computation or Fokker-Planck calculations. The synergy effect was found to vary with the radial location of EC power deposition, as predicted by kinetic theory. As shown in Fig. 9, F_{syn} values in the range of 1.3-4 are in very good agreement with the computed values using a 3-D Fokker-Planck code [39].

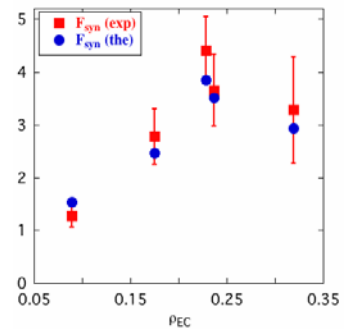


Fig. 9 : Synergy factor from experiment (squares) and from kinetic theory (dots)

3.6 Combined ICRH & LHCD experiments

Experiments combining ICRH and LHCD have been carried out. The highest injected energy reached so far was 430 MJ (3 MW, 65 s ICRH pulse during a 2 mn LHCD plasma). In these experiments, the temperature of the TPL was very stable. For example, during the application of a total power of 10 MW over 10 s (ICRH power \sim 8 MW), the TPL surface temperature reached its stationary value less than 550°C, corresponding to a thermal flux less than 5.7 MW/m².

In terms of confinement property, favourable characteristics occur during ICRH. Indeed, toroidal co-rotation (V_{Φ}) has been observed when the concentration of the resonating

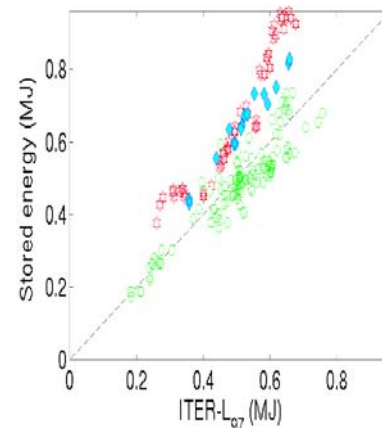


Fig. 10: Total energy versus thermal ITER L-mode prediction. Circles: L-mode plasmas), hexagons: Improved confinement ICRH plasmas.

minority ion is optimized ($n_{\text{H}}/n_{\text{e}} \approx 6\%$), correlating with an efficient bulk ion heating ($T_{\text{i}}/T_{\text{e}} \sim 1$) and an enhancement of energy confinement. The stored plasma energy (including fast ion

effects) exceeds the L-mode by a factor of 1.4-1.7. [40] (Fig. 10). Acceleration of the plasma in the toroidal co-current direction correlates well with the central ion pressure normalized to the plasma current [41]. The measurements of V_ϕ profile, by charge exchange recombination spectroscopy, indicated that the central V_ϕ value has reached 80 km/s [40]. As reported by Fenzi-Bonizec et al [40], Ion Temperature Gradient modes (ITG) and Trapped Electron Modes (TEM) inside $r/a = 0.6$ are stabilized by the $E \times B$ shear, through V_ϕ .

The origin of the toroidal plasma co-current rotation observed in ICRF heated plasmas in the absence of external momentum injection is not understood. Fast particle effects have been proposed [42-44], but the basic prediction of this theory is that co-(counter-) current rotation should arise when the ICRF resonance layer is placed on the low (high) field side of the magnetic axis. Since the observations of co-current rotation on Tore Supra have been made with high field side ICRF resonances, fast particle effects do not seem dominant. The accretion theory proposed by Coppi [45], could provide part of an explanation. It depends on the turbulent modes at the plasma edge, which are not yet well diagnosed on Tore Supra. A feature that somewhat distinguishes Tore Supra from JET and Alcator C-Mod, the other two machines where co-current rotation in the presence of ICRF heating has been observed, is its higher magnetic field ripple. It has been suggested that co-current rotation could be induced by a “ripple thermal force” [46-47], and the rotation velocities predicted are of the same order as those found in Tore Supra. However, more work is needed to quantify this effect in Tore-Supra case.

Generation of toroidal rotation without external torque is important in view of the ITER operation. Indeed, the torque produced by Neutral Beam Injection will be much reduced in ITER. Toroidal rotation is known to favour the formation of transport barriers and more generally leads to a reduction of turbulent transport via shear flow stabilization. It has also a beneficial effect on MHD stability, by preventing mode locking and the onset of Resistive Wall Modes. The values observed on Tore Supra have the right order of magnitude to act on MHD modes and turbulence. These are promising results for ITER, but a scaling of ICRH induced rotation is lacking.

3.7 Turbulent particle transport

The existence of anomalous particle pinch has been unambiguously proven in fully non-inductive Tore Supra discharges [48]. The electron density profile remains peaked in steady state over a time much longer than the current diffusion time (~ 80 times). This resilient peaked profile is explained by an inward pinch velocity two orders of magnitude above the expected neoclassical value. Two main mechanisms have been invoked to explain such a pinch [49-50]: i) turbulent thermodiffusion generating a pinch velocity, inward or outward, proportional to $\nabla T_e/T_e$; ii) magnetic field curvature leading to an inward pinch proportional to $\nabla q/q$ (also predicted by Turbulence Equi-Partition theory). The electron flux (Γ) is generally described by the following equation, including the Ware pinch (V_{Ware}) [51]:

$$\Gamma = -D [\nabla n_e + (C_q \nabla q/q - C_T \nabla T_e/T_e) n_e] + V_{\text{Ware}} n_e$$

The dependences on $\nabla T_e/T_e$ and on $\nabla q/q$, have been determined as functions of radial position in order to discriminate between the two main theoretical predictions mentioned above. For this, it is essential that the density profile be well diagnosed. This is the case in Tore Supra, thanks to powerful reflectometry with high temporal resolution ($\Delta t = 25 \mu\text{s}$) [52]. The results support the turbulent transport theories based on Ion Temperature Gradient (ITG) modes and Trapped Electron Modes (TEM). The main finding is that both curvature and thermodiffusion pinches co-exist [53]. The electron density profile is governed by $\nabla q/q$ and $\nabla T_e/T_e$ in full non-inductive discharges. However, the thermodiffusion pinch is found to be small. In the gradient region ($r/a = 0.3 - 0.6$), the electron density profile is mainly determined

by an inward pinch proportional to $\nabla q/q$, correlated with dominant unstable TEM, as predicted by transport simulations [49].

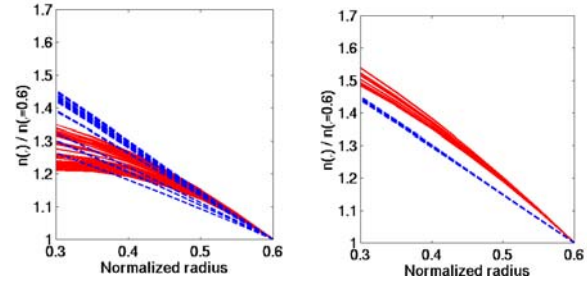
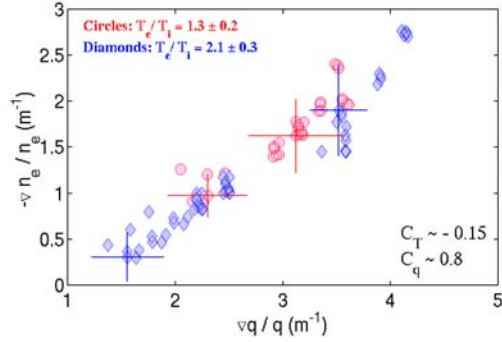


Fig. 11: $\nabla n_e/n_e$ versus $\nabla q/q$ within $0.3 \leq r/a \leq 0.6$ from a set of seven discharges, keeping $q_{edge} \sim 9$, right: $q_{edge} \sim 14$. Full experiments, $\nabla T_e/T_e$ at the value of $6 \pm 0.6 \text{ m}^{-1}$. Left: $q_{edge} \sim 9$, right: $q_{edge} \sim 14$. Full experiments, dashed: empirical model $\nabla n_e/n_e = 0.5 \nabla q/q$ [54].

The dependence of $\nabla n_e/n_e$ upon $\nabla q/q$ can be seen in Fig. 11. $\nabla n_e/n_e$ increases linearly as a function of $\nabla q/q$ with a positive slope corresponding to the coefficients $C_q = 0.8$ and $C_T = -0.15$. These coefficients indicate the inward pinches. Experimental n_e profiles seem to be determined by $\nabla n_e/n_e = 0.5 \nabla q/q$ (Fig. 12), in good agreement with an empirical model proposed Boucher et al [54].

In contrast, n_e profile peaking in the plasma core ($r/a \leq 0.3$), where unstable ITG modes dominate, is rather sensitive to the electron temperature gradient length when the Ware pinch is completely suppressed. $\nabla n_e/n_e$ versus $\nabla T_e/T_e$ is presented in Fig. 13. Best fits clearly show two regions. The direction of the thermodiffusion pinch is found to be inward in the inner plasma ($r/a \leq 0.3$), and outward in the outer plasma ($0.3 < r/a < 0.6$), i.e. the slope of the curves changes from negative to positive ($\nabla q/q$ is respectively 2 and 3.5). This change of direction is correlated with respectively dominant TEM and ITG modes, in agreement with turbulence simulation results in Ref [49].

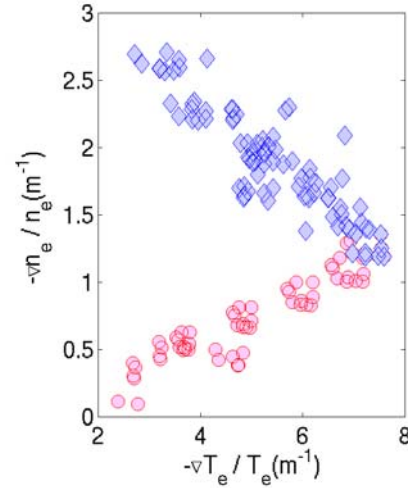


Fig. 13: $|\nabla n_e/n_e|$ versus $|\nabla T_e/T_e|$. Circles: $r/a \leq 0.3$, diamonds: $0.35 \leq r/a \leq 0.6$.

Anomalous pinch has beneficial effects on ITER operation. Indeed, a peaked n_e profile stabilizes ITG and Electron Temperature Gradient modes, and reduces heat transport. The Tore Supra results suggest a possibility to control these instabilities by controlling the density profile, through the q -profile, using an external non-inductive current drive method (for example ECCD or LHCD). A peaked density profile is moreover attractive to enhance the fusion power and the bootstrap current required for continuous operation.

Extrapolation to the ITER plasma performance has been simulated using the 0D module of the integrated code CRONOS. These simulations have been performed in a consistent manner using mixed empirical scalings (bootstrap current, radiated power, Z_{eff} ,...) [55]. In particular, we used the conservative scaling ITERH-98P(y,2) for global energy confinement [56]. In this simulation, the density peaking is assumed to be consistent with the condition $\nabla n_e/n_e = 0.5 \nabla q/q$, according to the results in Ref [54] and in Tore Supra (Fig. 12). Plasma dilution through possible impurity accumulation is not taken into account, but we include an increase

of Z_{eff} (from 1.55 to 1.7) which depends on the radiated power and on n_e using a scaling law based on JET results [57].

The results of simulations for ITER reference scenario with 40 MW of Neutral Beam Heating [4], as shown in Fig. 14, indicate that a fusion power of 530 MW ($Q \sim 13$) could be obtained with the effect of inward curvature pinch, to be compared with 400 MW ($Q = 10$) when using the flat density profile currently expected for ITER. Using a more favourable scaling, without beta dependence, as proposed in Ref [58], a large amount of fusion power is expected, but in this case, the gain due to the density peaking is smaller: 1.1 GW with a peaked n_e and 900 MW with a flat profile.

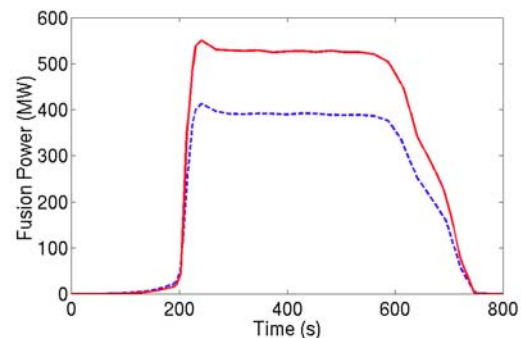


Fig. 14: Fusion power expected in ITER standard scenario from 0D CRONOS simulation. Dash: using flat n_e profile Full: with inward curvature pinch $\nabla n_e/n_e = 0.5 \nabla q/q$ [53], using the scaling ITERH-98P(y,2)

4. Conclusions

Tore Supra now operates routinely in steady-state, addressing novel issues both in physics and technology related to very long duration discharges. With regards to **steady state technology**, we first find that the use of superconducting coils is essentially trouble free since 14 years and is well adapted to Tokamak operation. Considerably more difficulties have been encountered with reliable steady state operation of plasma facing components, which requires a very precise knowledge of the distribution of power loading on all in-vessel components. These components need to be actively cooled accordingly and to be manufactured with essentially zero defect using high grade industrial quality control and comprehensive testing. These methodologies will be essential during ITER construction. With regards to **physics**, much has been learned from operating over very long time scales. Outstanding is the turbulent particle pinch effect which is projected to enhance ITER performance by about 30% and provides a new test of transport theories. Remarkable is also the subtle interplay between transport and current profile which can lead to slow oscillations and points to the importance of real time current profile control. In this area the synergy between the ECCD and LHCD waves appear promising. Finally the in-vessel hydrogen inventory which never saturates even over several minutes still poses unresolved questions. The presently **on-going upgrade** [59] of the 3 RF systems of Tore Supra to 600-1000s capability will allow increasing the operating domain contributing again to addressing ITER key steady state issues.

Acknowledgments

It is a pleasure to acknowledge the essential contributions to this work of the entire fusion research department (DRFC) in Cadarache and Drs Claudio De Michelis and Tuong Hoang who have greatly contributed to the edition of this article.

Reference

- [1] T. Fujita *et al*, Phys. Rev. Lett. 87 (2001) 245001
- [2] H. Zushi *et al*, Nucl. Fusion **43** (2003)1600
- [3] The JET Team, Proc. 15th Int. Conf. on Plasma Physics and Controlled Nuclear Fusion Research 1994 (Seville,1994) Vol 1 (Vienna: IAEA, 1995) 51
- [4] ITER, <http://www.iter.org/>
- [5] D. van Houtte *et al*, Nucl. Fusion **44** (2004) L11–L15
- [6] B. Beaumont *et al*, Fusion Engineering and Design, vol.56-57, 667-672 (2001)
- [7] P. Garin *et al*., Fusion Eng. Des. 56–57 (2001) 117

- [8] J. Schlosser *et al*, Fusion Eng. Des., vol 56-57 (2001) 309
- [9] A. Grosman *et al*, J. Nucl. Mater. 241-243 (1997) 618
- [10] D. Guilhem, *et al*, Proc. 30th EPS Conf. on Controlled Fusion and Plasma Physics (2003)
- [11] D. Guilhem, *et al*, Proc. 23rd SOFT Conference, Venice (Italy) (2004)
- [12] Y. Perrot *et al*, Proc. 23rd SOFT Conference, Venice (Italy) (2004)
- [13] Ph. Bibet *et al*, Proc. 20th SOFT Conference (1998) 339
- [14] F. Kazarian *et al*, Proc. 23rd SOFT Conference, Venice (Italy) (2004)
- [15] Ph. Bibet *et al*, Proc. 23rd SOFT Conference, Venice (Italy) (2004)
- [16] V. Pericoli *et al*, Proc. 31st EPS Conf. on Controlled Fusion and Plasma Physics (2004)
- [17] F. Durodié *et al*, Proc. 15th Top. Conf. On Radio Frequency Power in Plasmas, Moran (USA), (2003)
- [18] R. S. Hemsworth *et al*., Nucl. Fusion **43** (2003) 851
- [19] P. Massmann *et al*, Fusion Engineering and Design, vol.56-57 (2001) 539
- [20] C. Darbos *et al*, Proc. 23rd SOFT Conference, Venice (Italy) (2004)
- [21] J. Bucalossi *et al*, Proc. 19th IAEA Conference, Lyon (France) (2002)
- [22] A. Géraud, I. Viniar, S. Skoblikov *et al*, Fusion Engineering and Design 69 (2003) 5
- [23] P.T. Lang *et al*, Phys Rev Lett **79** (1997) 1487
- [24] V. Waller, B. Pégourié, G. Giruzzi *et al*., Phys Rev Lett **91** (2003) 205002
- [25] A. Géraud *et al*, 16th PSI (2004, Portland, USA), to be published in J. Nucl. Mater.
- [26] F. Saint-Laurent, 9th Int. Conf. on Accelerator and Large Exp.l Phys. Control Sys., Gyeongju, Korea (2003)
- [27] G.T. Hoang *et al*, Nucl. Fusion **34** (1994) 75
- [28] S.M. Kaye *et al*, Nucl. Fusion **37** (1997) 1303
- [29] V. Basiuk *et al*, Nucl. Fusion **43** (2003) 822.
- [30] E. Tsitrone *et al*, these proceedings
- [31] C. Brosset *et al*, 16th PSI (2004, Portland, USA), to be published in J. Nucl. Mater
- [32] D. Whyte *et al*, 16th PSI (2004, Portland, USA), to be published in J. Nucl. Mater
- [33] G. Martin *et al*, these proceedings
- [34] Maget P. *et al*, Nucl. Fusion **44** (2004) 443
- [35] Carreras B. *et al*., Nucl. Fusion **19** (1979) 583
- [36] G. Giruzzi *et al*, Phys. Rev. Lett. **91** (2003) 135001
- [37] F. Imbeaux *et al*, these proceedings
- [38] G. Giruzzi *et al*, these proceedings
- [39] G. Giruzzi, Plasma Phys. Control. Fus. **35** (1993) A123
- [40] C. Fenzi-Bonizic *et al*, 31st EPS Conf. on Controlled Fusion and Plasma Physics (2004), to be submitted to Plasma Phys. Control. Fus
- [41] L.-G. Eriksson *et al*, Nucl. Fusion, **41** (2001) 97
- [42] F.W. Perkins *et al*, Phys. Plasmas **8** (2001) 2181
- [43] V.S. Chan *et al*, Phys. Plasmas **9** (2002) 501
- [44] L.-G. Eriksson and F. Porcelli, Nucl. Fusion **42** (2002) 959
- [45] B. Coppi B., Nucl. Fusion **42** (2002) 1
- [46] A. B., Mikhailovskii, Plasma Physics Reports **21** (1995) 529
- [47] B. N Kuvshinov *et al*, Plasma Physics Reports **21** (1995) 713
- [48] G.T. Hoang, C. Bourdelle *et al*, Phys. Rev. Lett. **90** (2003) 155002
- [49] X. Garbet, *et al*, Phys. Rev. Lett. **91** (2003) 035001
- [50] X. Garbet *et al*, to appear in Plasma Phys. Control. Fus., Nov 2004.
- [51] A. A. Ware, Phys. Rev. Lett. **25** (1974) 916
- [52] R. Sabot *et al*, these proceedings
- [53] G.T. Hoang, C. Bourdelle *et al*, Phys. Rev. Lett. **93** (2004) 135003.
- [54] D. Boucher, P.H. Rebut *et al*, Academie Sciences. T315, Ser. II (1992) 273
- [55] G.T. Hoang *et al*, these proceedings
- [56] ITER Physics Basis, Nucl. Fusion, **39** (1999) 2208
- [57] G. F. Matthews, J. Nucl. Mater. 241-243 (1997) 618
- [58] D.C. McDonald *et al*, Plasma Phys. Control. Fus. **46** (2004) A215
- [59] B. Beaumont *et al*, Fusion Engineering and Design, vol.56-57 (2001) 667